JACS
JOURNAL OF THE AMERICAN CHEMICAL SOCIETY

ARTICLE

pubs.acs.org/JACS

Hydride-Induced Amplification of Performance and Binding Enthalpies in Chromium Hydrazide Gels for Kubas-Type Hydrogen Storage

Ahmad Hamaed,[†] Tuan K. A. Hoang,[†] Golam Moula,[†] Ricardo Aroca,[†] Michel L. Trudeau,[‡] and David M. Antonelli*[,†,§]

[†]Department of Chemistry and Biochemistry, University of Windsor, 401 Sunset Avenue, Windsor, Ontario N9B 3P4, Canada

[‡]Materials Science, Hydro-Québec Research Institute, 1800 Boul. Lionel-Boulet, Varennes, Québec J3X 1S1, Canada

[§]Sustainable Environment Research Center, University of Glamorgan, Pontypridd CF37-1DL, United Kingdom

Supporting Information

ABSTRACT: Hydrogen is the ideal fuel because it contains the most energy per gram of any chemical substance and forms water as the only byproduct of consumption. However, storage still remains a formidable challenge because of the thermodynamic and kinetic issues encountered when binding hydrogen to a carrier. In this study, we demonstrate how the principal binding sites in a new class of hydrogen storage materials based on the Kubas interaction can be tuned by variation of the coordination sphere about the metal to dramatically increase the binding enthalpies and performance, while also avoiding the shortcomings of hydrides and physisorpion materials, which have dominated most research to date. This was accomplished through hydrogenation of chromium alkyl hydrazide gels, synthesized from bis(trimethylsilylmethyl) chromium and hydrazine, to form materials with low-coordinate Cr hydride centers as the principal H_2 binding sites, thus exploiting the fact that metal hydrides form stronger Kubas interactions than the corresponding metal alkyls. This led to up to a 6-fold increase in storage capacity at room temperature. The material with the highest capacity has an excess reversible storage of 3.23 wt % at 298 K and 170 bar without saturation, corresponding to 40.8 kg H_2/m^3, comparable to the 2015 DOE system goal for volumetric density (40 kg/m^3) at a safe operating pressure. These materials possess linear isotherms and enthalpies that rise on coverage, retain up to 100% of their adsorption capacities on warming from 77 to 298 K, and have no kinetic barrier to adsorption or desorption. In a practical system, these materials would use pressure instead of temperature as a toggle and can thus be used in compressed gas tanks, currently employed in the majority of hydrogen test vehicles, to dramatically increase the amount of hydrogen stored, and therefore range of any vehicle.

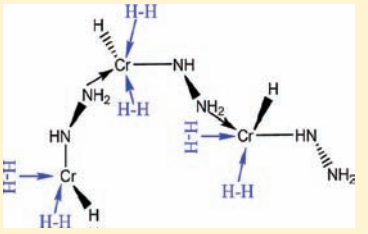

INTRODUCTION

Hydrogen is an ideal energy carrier because it contains more energy per gram than any other chemical substance.[1] However, its low density and high cost of compression have limited its applicability as a future energy provider. For this reason, a number of approaches have been developed using chemical substances as carriers. In these materials, hydrogen can be bound in the form of an M−H bond (metal hydride),[2] nested in interstitial sites in a metal alloy, or physisorbed to a surface.[3−6] However, metal hydrides have thermodynamic difficulties and slow kinetics of uptake and release,[7,8] alloys are expensive and possess low gravimetric capacities, while physisorption materials must be cooled to 77 K to be effective, making them impractical for on-board application. To date, none of these approaches have reached the 2015 DOE targets of 5.5 wt % and 40 kg/m^3.[9] An often overlooked feature of a hydrogen storage material is the enthalpy of binding. If this value is too high, as in metal hydrides, which generally possess enthalpies greater than 60 kJ/mol, large quantities of heat are released on charging, and external heating is required to drive the hydrogen off when required by the engine.[10,11] If the enthalpy is too low, as in physisorption materials, which generally possess enthalpies lower than 10 kJ/mol, the hydrogen does not adhere strongly enough to the material, and energy-consuming cryogenic temperatures are required.[3] Recent calculations predict that hydrogen bound in a Kubas fashion (i.e., a s−p bond in which electron density is back-donated from the metal d orbitals into the H−H antibonding orbital)[12] to a transition metal center should possess enthalpies of 20−30 kJ/mol, ideal for room temperature applications.[13−15] This was confirmed in our group by measurements on mesoporous silica materials with Ti(III) benzyl fragments grafted on the surface.[16] These materials possess enthalpies, which rise on surface coverage to 22 kJ/mol. This rising behavior is highly unusual and has been observed in our group on all materials where Kubas binding is proposed. The Ti(III) units on the silica surface can hold up to 4.0 H_2 per Ti at 77 K and 80 bar and 1.8 H_2 per Ti at 298 K and 80 bar, thus

Received: March 10, 2011
Published: August 24, 2011

retaining 40% of their activity and demonstrating that the higher enthalpies of binding indeed improve room temperature performance. The major drawback of these materials is that the percentages of Ti are low (ca. 5%), the surface metal fragments are unstable over time, and the majority of hydrogen is still bound by traditional physisorption.[16] For this reason, materials with much higher percentages of the crucial transition metal must be synthesized. Such materials must possess metals in low oxidation states for effective back-donation into the H−H antibonding orbital. The metal must also be in a low coordinate environment to allow maximum hydrogen binding, and the metal and support structure must also be light, so as not to affect gravimetric performance, while being porous enough for hydrogen diffusion without creating excess void space. In 2010, we reported new Cr and V hydrazide gels, which use hydrazine as a linker to incorporate a high concentration of low coordinate transition metal sites useful for Kubas binding.[17,18] These materials were synthesized by condensation of hydrazine with a transition metal complex accompanied by concomitant loss by protonolysis of the hydrocarbon ligand. The resulting amorphous solids possess linear isotherms, enthalpies that rise on surface coverage to 45 kJ/mol and retain up to 49% of their adsorption at room temperature as opposed to 77 K. For this reason, they must be considered a new class of hydrogen storage materials distinct from hydrides and physisorption materials. However, these materials still fall short of practical applications, possibly because the residual ligand from the precursor (Cp, mesityl, or THF) remains in the structure, blocking coordination sites that could be used for hydrogen binding. In this Article, we show how residual alkyl groups in related Cr hydrazide gels can be hydrogenated off to form Cr−H centers, which form much stronger Kubas interactions than the corresponding Cr alkyl. This leads to a dramatic increase in binding enthalpies and room temperature performance, with some materials surpassing the 2015 DOE goal for volumetric density at 298 K.

EXPERIMENTAL SECTION

Chemicals were purchased from Aldrich and used as is, with the exception of $CrCl_3$, which was thoroughly ground in an oven-dried mortar and pestle under Ar before use. All solvents were distilled over sodium/benzophenone before use. Manipulations were performed in an Ar glovebox as low-valent early transition metal species are often sensitive to air, moisture, and often dinitrogen.

Preparation of Bis[(trimethylsilyl) methyl]chromium(II) or $Cr_4(CH_2Si(CH_3)_3)_8$.[19] To a stirred suspension of $CrCl_3$ (4.8 mmol) in hexane was added a solution of $(CH_3)_3SiCH_2Li$ (14.4 mmol) also in hexane. The color of the slurry changed to dark purple after several hours. The mixture was stirred at room temperature for 4 h, then filtered, and the residue was washed with three portions of hexane (10 mL each). The solution and washings were concentrated to 50 mL and allowed to stand at −34 °C for 12 h. The color of the solution slowly turned brown upon standing, and crystals formed. The solid product was isolated by cold filtration, washed twice with precooled hexane, and dried in vacuo.

Preparation of Anhydrous Hydrazine. Pure hydrazine was prepared from hydrazine monohydrate by azeotropic distillation with toluene to remove water and avoid possible explosion.[20] 100 mL of hydrazine monohydrate and 250 mL of toluene were added to a 500 mL one neck round-bottom flask, equipped with a thermometer to measure the gas temperature. Hydrazine is toxic, corrosive, and flammable; it should be handled with extreme care.[20] A water condenser was connected, and 2 flashes were collected and discarded before collecting the hydrazine fraction. After distillation and removal of water, 35 g of NaOH was added to the hydrazine−toluene flask, and the hydrazine was distilled under vacuum.

Preparation of 1:1 Chromium Hydrazide Gel (Cr−MHz (1.0)). In a typical synthesis, Cr−MHz (1.0) was synthesized as follows: bis[(trimethylsilyl) methyl]chromium (6.50 g, 31.64 mmol) was dissolved in 150 mL of dry toluene at room temperature in a Schlenk tube under Ar. 1.014 mL of hydrazine (1.014 mL, 31.64 mmol) was then added by syringe with vigorous stirring. The stirring was continued for 24 h. The solution was then heated to 50 °C for 24 h, to 80 °C for 24 h, and to 100 °C for another 24 h with stirring. After this, the suspension was filtered, and a black solid was obtained with a colorless filtrate, indicating complete precipitation of all Cr species. This solid was washed with hexane and then transferred to an air-free tube and divided into 3 aliquots to test the effect of further heating on hydrogen storage performance. One aliquot was dried at room temperature under vacuum for 4 h, while the other two aliquots were dried by heating at 100 °C for a period of 8 h for one of them and at 150 °C for 8 h for the other.

Preparation of Cr−MHz (0.5), Cr−MHz (1.5), and Cr−MHz (2.0). The same procedure was followed as with Cr−MHz (1.0) for the preparations of Cr−MHz (0.5), Cr−MHz (1.5), and Cr−MHz (2.0), but with 0.507, 1.521, and 2.028 mL of hydrazine, respectively.

Hydrogenation of Cr−MHz Materials. The hydrogenation of all chromium hydrazide samples was conducted by treating the sample loaded onto the sample chamber of a gas reaction controller (GRC) with pure hydrogen for 4 h at 85 atm and 180 °C. This optimal hydrogenation condition was obtained by running a series of hydrogenation reactions at 100 °C and 85 atm for 2 h; at 100 °C and 85 atm for 24 h; at 150 °C and 85 atm for 4 h; at 180 °C and 85 atm for 4 h; and at 200 °C and 85 atm for 4 h. The reaction was monitored by observing the hydride and C−H regions of the infrared spectrum (IR). The relative intensity of the C−H stretching vibration observed at 2800 cm^{-1} decreases, and a new absorption band assigned to a Cr−H moiety appears at 2050 cm^{-1}. The hydrogenation reaction is considered complete when the relative intensity of the original C−H stretching vibrational band approaches the noise level.

Characterization. Nitrogen adsorption and desorption data were collected on a Micromeritics ASAP 2010. Powder X-ray diffraction (XRD) was performed on Siemens D-500 diffractometer with Cu Kα radiation (40 KV, 40 mA) source. The step size was 0.02°, and the counting time was 0.3 s for each step. Diffraction patterns were recorded in the 2θ range 2.3−52°. Samples for XRD analysis were put in a sealed capillary glass tube to protect sample from air and moisture during experiment. All X-ray photoelectron spectroscopy (XPS) peaks were referenced to the carbon C−(C, H) peak at 284.8 eV, and the data were obtained using a Physical Electronics PHI-5500 spectrometer. Charge neutralization was not necessary, suggesting that the materials are metallic. Elemental analysis was conducted at Galbraith Laboratories, Knoxville, TN.

Infrared Spectroscopy. Infrared spectroscopy was conducted on a Bruker Vector 22 instrument. In a typical experiment, 7 mg of sample was mixed with 600 mg of dry KBr, and a pellet was made in a dry argon box. The pellet was then transferred to the IR instrument in a capped vial, and the measurement was conducted immediately.

Raman Spectroscopy. Samples were loaded in NMR tubes fitted with Young's valves, and spectra were recorded at 1 atm H_2, D_2, or Ar. For the spectra recorded after vacuum, the samples were left for 1 h under H_2 or D_2 and then placed under vacuum for 10 min before backfilling with Ar. All micro-Raman scattering experiments were conducted using a Renishaw InVia system, with laser excitation at 514.5 nm, and powers of 10−20 μW at the sample. Each scan was duplicated to ensure that any features observed were reproducible. All measurements were made in a backscattering geometry, using a 20× microscope objective with a numerical aperture value of 0.40, providing scattering areas of ∼20 μm^2. Single-point spectra were recorded with

4 cm^{-1} resolution and 50 s accumulation times. Data acquisition and analysis were carried out using the WIRE software for windows and Galactic Industries GRAMS C software.

Hydrogen Adsorption Measurements. Hydrogen adsorption isotherms were obtained by using a computer-controlled commercial Gas Reaction Controller manufactured by Advanced Materials Corporation, Pittsburgh, PA, except in the case of the isotherm recorded at 170 bar, which was obtained on a Hy-Energy PCT Pro. High purity hydrogen (99.9995% purity) was used as the adsorbent. All measurements were performed exactly as reported previously by our group to ensure reproducibility.[16] Skeletal densities were collected using a Quantachrome Ultrapycnometer housed in an Ar glovebox. This instrument is calibrated bimonthly as per user manual, using a small sphere with a known volume of 0.0898 cm^3 to monitor the instrument's performance. The volume of an empty cell is collected over several running cycles using He until the values are within ±2% difference. A preweighed portion of sample is loaded into the cell under inert conditions, and the volume of the system (sample + cell) is then determined. The skeletal volume of the sample is the difference between volume of sample + cell and the volume of empty cell. Skeletal density is obtained by using the sample mass divided by the sample volume. Excess hydrogen storage measurements on a standard AX-21 sample (4.2 wt % at 30 bar and 77 K, 0.55 wt % at 80 bar and 298 K) were performed to ensure proper calibration (please see Figure S1, Supporting Information). Heat of hydrogen adsorption on carbon AX-21 was provided in Figure S2.[17] Leak testing was also performed during each measurement by checking for soap bubbles at potential leak points. These measurements are all necessary to ensure the veracity of the isotherms. In the H_2 adsorption−desorption experiments, a high level of reversibility was observed for all samples across the whole range of pressures. Samples were run at liquid nitrogen temperature (77 K), liquid argon temperature (87 K), and room temperature (298 K) to 85 bar on the Advanced Materials instrument and up to 170 bar on the PCT Pro. Isotherms were always measured first at room temperature and then at 77 or 87 K, and the temperature was kept constant by keeping the sample chamber in liquid N_2, liquid Ar, or water. In the Advanced Materials instrument, the sample weight and skeletal density are used to determine the volume of the sample in the sample chamber, which is then subtracted from the sample chamber volume to provide an accurate void space volume. When the skeletal density is used for the gravimetric hydrogen uptake measurement, the compressed hydrogen within the pores is treated as part of the sample chamber volume and hence subtracted. Therefore, only the hydrogen contained on or beneath the walls of the structure will be recorded by the PCI instrument. This gravimetric value is termed the adsorption or excess storage. When the bulk density is used, the hydrogen in the pores of the sample is automatically included in the calculation without any further correction factors, and the final value is termed the total storage[21] or absolute storage,[22] which represents all hydrogen contained in the sample including the compressed gas in the voids and the hydrogen adsorbed on or beneath the walls of the structure. Gravimetric densities are recorded as read from the isotherms, while volumetric densities are calculated from the adsorption data and the skeletal or bulk density, depending on the desired value. The excess volumetric storage is typically calculated from the excess storage and the bulk density and gives a measure of the gas adsorbed on or in the solid phase of the material scaled across the entire volume occupied by the sample including the void space. In materials such as MOFs that possess a well-defined and constant ratio between mass and void space, this value is often quoted. For compressible materials that may have variable ratios of solid mass and void space, it can often help to scale the volumetric density to the solid phase alone as the void space will vary on sample preparation. For this purpose, we have defined the true volumetric adsorption[18] as the amount of hydrogen adsorbed on or in a given volume of the solid portion of the sample. This is calculated from the excess storage data and the skeletal density. This value neglects the void space and is useful in comparing volumetric densities of ball-milled powders and gels (materials with textural porosity only and no intrinsic pore structure) to pure solid phase materials such as metal hydrides. Because the materials in this study stand between hydrides and physisorption materials in their mechanism of storage, this value is important. It also allows us to compare volumetric adsorption values of the solid phase alone from one sample to another without having to correct for the different textural void space in each material. The absolute volumetric adsorption has also been defined[22] and is a representation of the sum of the excess volumetric storage plus the compressed gas in the void space. This can be calculated from the volumetric storage as measured from the instrument and the bulk density, or by taking the volumetric adsorption and adding on the amount in the void space calculated from the pore volume and the ideal gas law.[21] The first method is only possible when using the Advanced Materials instrument. In this Article, we have chosen not to calculate this value (or the total gravimetric storage) because the differences between the skeletal densities and bulk densities are much smaller than in MOFs, and hence the void space compressed gas contribution is negligible and will also vary due to sample preparation.

Enthalpies of adsorption were calculated using a variant of the Clapeyron−Clausius I equation taking both 77 and 87 K hydrogen excess storage data.[23] Pressure as a function of the amount adsorbed was determined by using exponential fit for each isotherm; the first 10−11 points of the isotherms were picked up and fit to the exponential equation. This exponential equation provides an accurate fit over the pressure up to 1 MPa with the goodness of fit (R^2) above 0.99. The corresponding P_1 and P_2 values at a certain amount of H_2 adsorbed at both temperatures can be obtained by the simulated exponential equation. Inputting these numbers into eq 1, we then calculate the adsorption enthalpies. This technique is commonly used to measure enthalpies of amorphous carbons and MOFs. Because the enthalpy of a reaction does not vary with temperature, unlike Gibbs free energy, this method provides information on hydrogen binding that is meaningful over a wide temperature range.

H_2/Cr Calculations. Calculations on hydrogenated samples were based on elemental analysis data from Table S1. As an example calculation, H_2−Cr−MHz (1.5) absorbs 3.23 wt % of hydrogen at 170 bar and 298 K. This corresponds to 3.23 g or 1.62 mol of H_2 for each 100 g of sample. Based on the 53.03% Cr in the sample from Table S1, this translates into 1.75 mol of H_2 per chromium center.

RESULTS AND DISCUSSION

Bis[(trimethylsilyl) methyl] chromium(II) was stirred with various amounts of anhydrous hydrazine in dry toluene with heating from 20 to 100 °C over several days to yield a series of air sensitive black solids. The molar ratio of bis[(trimethylsilyl) methyl]chromium(II) to hydrazine was varied according to the ratios 2:1, 1:1, 1:1.5, and 1:2, and the as-synthesized Cr- hydrazide samples were given the following annotations: Cr−MHz (0.5), Cr−MHz (1.0), Cr−MHz (1.5), and Cr−MHz (2.0), corresponding to hydrazine-to-Cr molar ratios of 1:2, 1:1, 1.5:1, and 2:1, respectively. The reaction mixture was then filtered under argon, and the dark solid obtained was split into 3 aliquots to determine the optimal drying conditions before characterization and further study of hydrogen storage properties. The first aliquot was dried at room temperature under vacuum for 4 h. The second was dried at 100 °C, under vacuum for 8 h, and the third aliquot was dried under vacuum at 150 °C, for 8 h. The skeletal density of each sample was then determined, and the excess hydrogen storage capacity was measured. From the four sets of results, it was obvious that drying at 100 °C for 8 h

Table 1. Summary of Excess Storage Results on Chromium Hydrazide Materials Dried at 100 °C before and after Hydrogenation[a]

material	BET surface area (m^2/g)	skeletal density (g/cm^3)	gravimetric adsorption (wt %)	volumetric adsorption (kg/m^3)	retention at 298 K (%)
Cr−MHz (0.5)	221	1.32	1.39 (at 77 K)	18.35 (at 77 K)	73
			1.01 (at 298 K)	13.33 (at 298 K)	
H2−Cr−MHz (0.5) "Cr_2N"	181	1.86	2.28 (at 77 K)	42.41 (at 77 K)	62
			1.41 (at 298 K)	26.23 (at 298 K)	
Cr−MHz (1.0)	210	1.47	2.02 (at 77 K)	29.69 (at 77 K)	21
			0.42 (at 298 K)	6.17 (at 298 K)	
H2−Cr−MHz (1.0) "CrN_2H_2"	171	1.47	2.05 (at 77 K)	30.13 (at 77 K)	80
			1.65 (at 298 K)	24.25 (at 298 K)	
Cr−MHz (1.5)	276	1.64	2.05 (at 77 K)	33.62 (at 77 K)	13
			0.26 (at 298 K)	4.264 (at 298 K)	
H2−Cr−MHz (1.5) "CrN_3H_4"	208	1.93	1.87 (at 77 K)	36.09 (at 77 K)	83
			1.55 (at 298 K)	29.92 (at 298 K)	
Cr−MHz (2.0)	374	1.41	3.47 (at 77 K)	48.93 (at 77 K)	14
			0.48 (at 298 K)	6.77 (at 298 K)	
H2−Cr−MHz (2.0) "CrN_4H_6"	203	1.65	1.23 (at 77 K)	20.29 (at 77 K)	100
			1.41 (at 298 K)	23.26 (at 298 K)	

[a] Data taken at 85 bar.

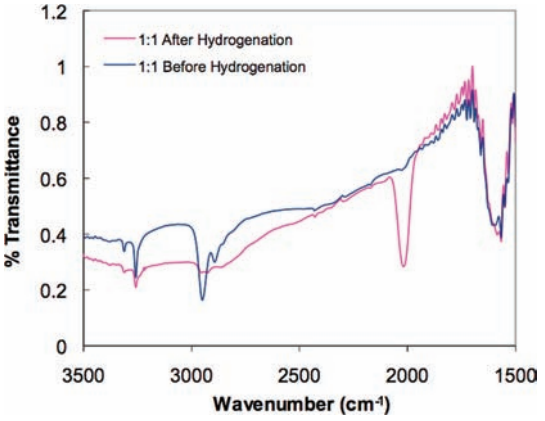

Figure 1. Infrared spectra of Cr−MHz (1.0) before (blue) and after (pink) hydrogenation at 180 °C and 85 atm for 4 h.

under vacuum was optimal. For example, for Cr−MHz (2.0), the excess storage at 77 K and 80 bar was 2.01, 3.47, and 2.79 wt % for room temperature, 100 °C, and 150 °C, respectively. A summary of the results of the materials dried at 100 °C is shown in Table 1. On the other hand, heating to 150 °C under Ar led to a collapse of the gel structure as confirmed by BET surface area measurements. For instance, the BET surface area of Cr−MHz (2.0) decreases from 374 to 279 m^2/g as the drying temperature increases from 100 to 150 °C. Nitrogen adsorption isotherms for the four materials dried at 100 °C recorded at 77 K are shown in Figure S3. These Type II isotherms exhibit a small amount of microporosity comprising roughly 20% the total volume adsorbed, with additional mesoporosity and textural porosity accounting for the remaining adsorption in roughly equal proportions as evidenced by the slow rise from 0.2 to 0.8 P/P_0 and the sharp incline above 0.8 P/P_0, respectively. The XRD powder patterns of Cr−MHz (0.5), Cr−MHz (1.0), Cr−MHz (1.5), and Cr−MHz (2.0) are shown in Figures S5−S8 and demonstrate that these materials are largely amorphous. There are also broad low-intensity reflections from 30 to 35 2θ that do not correspond to any known Cr−N phase. This is surprising because previously studied V(III) hydrazide gels were totally amorphous with no sign of any ordered phase in the XRD.[18] Figure 1 and Figures S9−S11 show the infrared spectra of these same Cr-based materials. From the large C−H stretch at 2800 cm^{-1} in all spectra, it is clear that the protonolysis reaction did not go to completion. There is also a large absorbance for an N−H stretch from 3200 to 3300 cm^{-1} and a small absorbance at 2050 cm^{-1} observed in Cr−MHz (1.0) and Cr−MHz (1.5) only corresponding to an M−H stretch, likely formed by α-migration of an N−H to the Cr center. This reaction is common in low-coordinate, low-valent early transition metal species containing an α-hydrogen.[23] It is not clear why the hydride migration only occurs in the 1.0 and 1.5 materials; however, a possible explanation may be a combination of the steric hindrance of the bulky alkyl group and lack of available hydrazide N−H protons in Cr−MHz (0.5), and an excess of hydrazine N-donors blocking the open Cr coordination sites that would otherwise be available for α-migration in the 2.0 material.

The X-ray photoelectron spectra of these materials are shown in Figures S12, S14, S16, and S18. The Cr 2p region shows a major emission that can be simulated as a mixture of three smaller emissions, the 3/2 components falling at 575.1, 577.6, and 578.8 eV, respectively. These emissions are consistent with a mixture of Cr(II) and Cr(III) sites by comparison with the corresponding cyclopentadienyl Cr(II) hydrazide gels published previously by our group,[17] although direct comparisons are not possible due to the different electronic effects of the cyclopentadienyl group as compared to the trimethylsilyl methyl group. There is also an emission in Cr−MHz (1.0) and Cr−MHz (1.5) at 580.5 eV corresponding to Cr (IV). This peak likely corresponds to the Cr centers in the small amount of Cr−H observed by IR in these materials, proposed to have formed by oxidative migration of an α-hydrogen onto Cr(II) to make a Cr(IV) hydride. The N1s region of the XPS spectra of these materials can be simulated as a mixture of four species at 396.2, 397.4, 398.1, and 400.2 eV, with

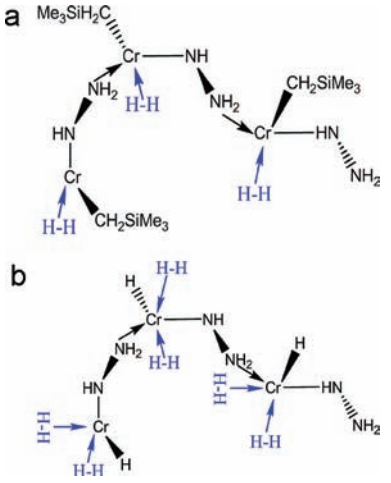

Figure 2. (a) Proposed structure of Cr−MHz (before hydrogenation) showing H_2 binding sites. (b) Proposed structure of Cr−MHz (after hydrogenation) showing H_2 binding sites.

the species at 397.4 eV having the highest intensity. Previous work on metal hydrazides[17,18] has shown that in general the energy of the N1s emission in bound M_xNH_y species increases as M is substituted for H and also as the coordination number of N increases from 3 to 4. Thus, the emission at 396.2 eV likely corresponds to a Cr−N−Cr species created by a double protolysis or a Cr═N species formed by a single protolysis followed by an α-migration of the remaining N−H to the metal center to form a Cr−H. On the basis of increasing eV with substitution of M for H on N, the main peak at 397.4 eV can be assigned to a Cr−**N**H−N species, while the emission at 400.2 eV is attributed to a terminal **N**H_2−NH−Cr species and the emission at 398.1 eV is assigned to a quaternary Cr−**N**H_2−N species. There is also an emission at 394.3 eV in Cr−MHz (1.0) only, which possibly corresponds to a hydrazine N bridging three Cr centers. On the basis of these data, a proposed molecular structure for the Cr−MHz products of the reaction of bis[(trimethylsilyl) methyl] chromium(II) with hydrazine is shown in Figure 2a.

The excess storage isotherms at 298 K up to 85 bar for the Cr−MHz materials prepared with various Cr-to-hydrazine molar ratios are shown in Figure 3a. These isotherms show little increase in excess storage with pressure up to about 25 bar. After 25 bar, the H_2 uptake increases more sharply with pressure, rising in a linear fashion. The excess storage reaches 1.01 wt % for the Cr−MHz (0.5), and 0.42, 0.26, and 0.48 wt % for the Cr−MHz (1.0), Cr−MHz (1.5), and Cr−MHz (2.0), respectively (Table 1), without saturation. The isotherms return on desorption to zero with only a slight hysteresis at low pressure. Repeat adsorption isotherms of the same sample are identical to the initial adsorption, demonstrating that this hysteresis is kinetic in nature, possibly due to a small amount of bound H_2 remaining in the structure that can readily be removed by vacuum. The excess hydrogen storage isotherms at 77 K for these materials are shown in Figure 3b and range from 3.47 wt % for the Cr−MHz (2.0) to 1.39 wt % for Cr−MHz (0.5). The excess storage retention of these materials at room temperature reaches 72% in the case of Cr−MHz (0.5). This is the highest retention of performance value ever recorded on going from 77 to 298 K. However, the absolute values are still lower than corresponding V(III) hydrazide gels, which show up to 4.04 wt % at 77 K and 85 bar and 1.17 wt % at 298 K and 85 bar.[18] The skeletal densities of these Cr materials range from 1.64 to 1.32 g/cm^3, while the BET surface areas range from 210 to 374 m^2/g. A complete summary of all data related to these materials is shown in Table 1.

The hydrogen binding enthalpies of the as-synthesized Cr−MHz samples (Figure 4) rise with the hydrogen loading level up to a maximum of 17.8 kJ/mol in the case of Cr−MHz (0.5). The rising trend in enthalpies with loading is characteristic of all materials studied by our group in which the Kubas interaction is proposed as the primary binding mechanism.[16−18] This was supported by computational studies[25] and was attributed to a sequential decrease in positive charge at the metal with H_2 ligation. The decreasing positive charge improves the π-bonding from the metal d-orbitals into the H−H antibonding orbital, hence increasing the binding enthalpy. Thus, while physisorption assumes a static surface during progressive adsorption of H_2, leading to the typical downward trend in enthalpy with surface coverage as the sites of highest enthalpy are occupied first, the average binding enthalpy of the sites in our materials increases with increased H_2 ligation at the metal as the surface changes with hydrogen exposure. The other Cr−MHz samples have rising binding enthalpies ranging from 2.55−12.54, 1.87−11.22, and 2.55−5.03 kJ/mol for Cr−MHz (2.0), Cr−MHz (1.0), and Cr−MHz (1.5), respectively. On inspection, these enthalpies bear a direct relationship with the room temperature excess storage, as the higher is the upper range of the binding enthalpy, the higher is the excess storage capacity at 298 K. For example, Cr−MHz (0.5) possesses both the highest excess storage in the series at 298 K (1.01 wt %) and the highest enthalpy maximum (17.8 kJ/mol). At 77 K, the situation is different as Cr−MHz (0.5) has the lowest performance of the series (1.39 wt %), with Cr−MHz (2.0) possessing the highest excess storage under these conditions (3.47 wt %). This suggests that enthalpy controls the relative retention of storage from 77 to 298 K, but the absolute value of the excess storage also depends on other factors such as the number of binding sites and their relative accessibility. Thus materials with low enthalpies and a high concentration of binding sites may outperform samples with higher enthalpies and fewer binding sites at 77 K, but this trend could be reversed at 298 K.

Computational studies on low coordinate transition metal fragments supported on silica, metal hydrazides,[25] and experimental investigations on H_2 binding to transition metals[12] have demonstrated that M−H moieties are more effective at hydrogen binding than are M−R, where R is a bulky alkyl or aryl ligand. Because of this, replacing the residual alkyl groups in the Cr−MHz materials with hydride ligands should increase the affinities of the corresponding Cr sites for H_2 while also reducing the weight of the material and possibly opening up new Cr sites previously blocked by the bulky trimethylsilyl methyl ligand. On this theme, different hydrogenation conditions were applied to a series of Cr−MHz (1.5) aliquots to arrive at the optimal condition for the substitution of the trimethylsilyl methyl ligand with hydride by σ-bond metathesis, and the reaction was monitored by observing the decrease in the C−H stretch in the IR spectrum before and after hydrogen treatment. A small quantity of Cr−MHz (1.5) was thus loaded into the gas reaction controller (GRC), and the sample was soaked with H_2 at an initial pressure of 5 atm, after which the temperature was set to 100 °C and the pressure gradually increased to 85 atm. The sample was left at 85 atm and 100 °C for 2−4 h, and then the IR spectrum of the hydrogenated sample was measured, followed by

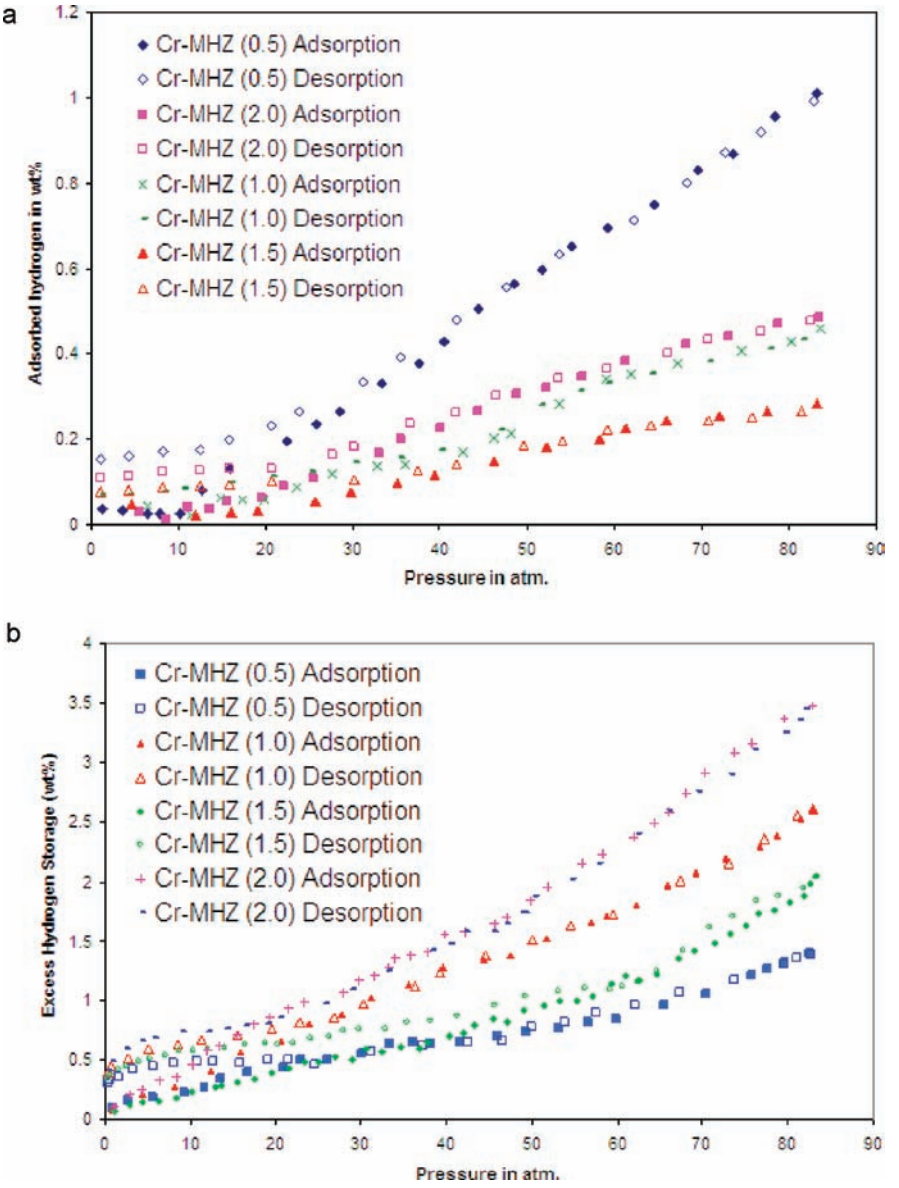

Figure 3. (a) Excess storage isotherms at 298 K for the as-synthesized Cr—hydrazide samples prepared with various Cr:N_2H_4 ratios before hydrogenation. (b) Excess storage isotherms at 77 K for the as-synthesized Cr—hydrazide samples prepared with various Cr:N_2H_4 ratios (samples were dried at 100 °C).

the excess hydrogen storage capacity. After this procedure was repeated in 20 °C increments up to a maximum temperature of 200 °C, it was found that 4 h hydrogenation at 180 °C was the optimal protocol for hydrocarbon loss as confirmed by a large decrease in the intensity of the C—H stretch accompanied by the appearance of a new Cr—H stretch at 2050 cm^{-1}, coinciding exactly with the Cr—H peak in the unhydrogenated 1.0 and 1.5 samples. While a very minor amount of hydrocarbon still remained in the sample as evidenced by IR, temperatures higher than 180 °C lead to a diminishing of the hydrogen storage capacity and loss of surface area.

These optimal hydrogenation conditions were applied to the other three Cr—MHz samples, and the IR spectra before and after reaction are shown in Figures S9—S11. The XRD patterns of the hydrogenated materials are shown in Figures S5—S8, revealing the presence and increase in intensity in all samples of the crystalline phase observed in the 1.0 and 1.5 samples before hydrogenation. This and the loss of BET surface areas (Table 1) suggest a phase change on heating and hydrogenation accompanied by densification of the structure. Elemental analysis is shown in Table S1 versus the theoretical values for the hydrocarbon-free samples on the basis of stoichiometries calculated assuming complete reaction. In all cases, the Cr value is somewhat lower than expected, similar to the ICP data we have obtained for other hydrazides made by our group,[17,18] and attributable to incomplete digestion of the Cr material. The presence of residual carbon ranging from 5.11% to 7.89% in these samples indicates that hydrogenation was not effective in removing the last traces of hydrocarbon, possibly due to trapping of the tetramethylsilane byproduct in the pore structure. The nitrogen values are also lower than expected, likely due to the combination of residual hydrocarbon and nitride formation on combustion,

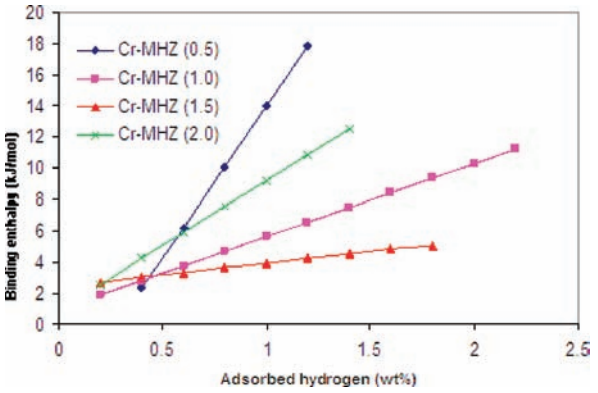

Figure 4. Binding enthalpies for the as-synthesized chromium hydrazide samples prepared with various Cr:N_2H_4 ratios before hydrogenation.

which has been observed in our previous hydrazide materials[17,18] and is often observed in the elemental analysis of early transition metal organometallics.

The X-ray photoelectron spectra of these hydrogenated materials are shown in Figures S13, S15, S17, and S19. The Cr 2p region of the XPS spectra of all materials is remarkably similar to those of the unhydrogenated materials with the exception that the emission at 580.5 eV in the 1.0 and 1.5 samples disappears, consistent with reduction of the Cr(IV) species. Examination of the N1s region reveals that the hydrogenation reaction increases the intensity of the emission at 397.4 eV over that at 396.2 eV, with the emission at 394.3 eV in Cr−MHz (1.0) disappearing completely, while the other emissions appear relatively unaffected. On the basis of our previous assignments, this is consistent with the hydrogenation of a bridging or terminal Cr imido to an amido Cr−H species. Figure 2b illustrates a proposed structure of the chromium hydrazide gels after complete hydrogenation.

The excess storage isotherms of the hydrogenated chromium hydrazides are shown in Figure 5a (298 K) and Figure 5b (77 K). These values reach as high as 1.65 wt % at 298 K and 85 bar for H_2−Cr−MHz (1.0), equating to a true volumetric density of 24.27 kg/m^3 (for a full explanation of volumetric densities, see the Experimental Section). H_2−Cr−MHz (1.5) absorbs 1.55 wt % under the same conditions, corresponding to a true volumetric density of 29.92 kg/m^3. These values are roughly 3 times that of compressed gas and compare to a value of 10.92 kg/m^3 for MOF-177 under the same conditions.[26] They are also much greater than those for the unhydrogenated hydrazides, demonstrating the profound effect of hydrogenation on the hydrogen storage performance at room temperature. For example, the hydrogenated Cr−MHz (1.5) possesses an excess storage of 1.55 wt %, which is roughly 6 times its excess storage capacity before hydrogenation. It is also apparent that hydrogenation has a much less pronounced effect on the excess storage at 77 K, and for Cr−MHz (1.5) and Cr−MHz (2.0), this process actually decreases it. Another obvious trend is that the percentage of retention of excess storage capacity at 298 K relative to 77 K increases in the series from 62% to over 100% with increasing hydrazine concentration. In fact, Cr−MHz (2.0) absorbs 1.41 wt % at 298 K and 85 bar and only 1.23 wt % at the same pressure and 77 K. The reason for these observations is not known at this stage, but may be due to the equilibrium thermodynamics of hydrogen binding in the different ligand environments at different temperatures. Similar to other hydrazides made by our group,[17,18] these isotherms are also linear and do not saturate at 85 bar at 77 or 298 K. This suggests that the excess storage values may be even higher at elevated pressures. Although the DOE suggests 100 bar as a target, the pressure of 200 bar defines the upper limit of safe storage for transportation in a conformable hydrogen cylinder, and it is conceivable that these materials may possess excess storage values as high as 2.5 times their values at 80 bar under these conditions. Thus, a pellet was made by compressing H_2−Cr−MHz (1.5) at 2500 psi, and the excess storage up to 170 bar was measured (Figure 5c). This material absorbs 3.2 wt % at room temperature reversibly without saturation with an absolute room temperature volumetric density of 40.8 kg/m^3 (calculated from an apparent density for the pellet of 1.275 g/cm^3), surpassing the 2015 DOE goal for volumetric density, although this goal is defined for a system and not just a chemical sorbent in isolation. For comparison, this value is greater than that of compressed gas at 77 K and 85 bar (28.05 kg/m^3), without the disadvantage of the energy loss incurred from cooling.[26] The excess storage of this same compressed sample at 298 K and 85 bar is 1.6 wt %, almost exactly the same as the value for this material from Figure 4b, indicating that performance was not lost on compression of the powder into pellet form, as observed for the related V(III) hydrazide.[18] The value of 3.2 wt % is not surprising given that Cr−MHz (2.0) absorbs 3.5 wt % without saturation at 80 bar and 77 K. In this system, the higher pressure is used in place of lower temperature to fill the open Kubas coordination sites. The excess storage value at 170 bar corresponds to 1.75 H_2/Cr, less than the 3 H_2 per Cr maximum expected for a tetrahedral CrL_2X_2 center according to the 18-electron rule. For comparison, on the basis of the calculated formula of CrN_3H_4 (Table S1), this maximum of 3 H_2/Cr would lead to a gravimetric performance of ca. 6 wt %. The surprisingly small difference between the apparent density and skeletal density of this material is consistent with the low surface area of this material and the large degree of textural porosity created by spaces between the particles, which themselves possess only a small amount of microporosity.

The binding enthalpies of the hydrogenated samples increase more steeply with H_2 loading than those of the unhydrogenated samples (Figure 6), reaching 22.9, 22.1, 50.24, and 51.58 kJ/mol for H_2−Cr−MHz (2.0), H_2−Cr−MHz (1.5), H_2−Cr−-MHz (1.0), and H_2−Cr−MHz (0.5), respectively. The largest increase in the peak enthalpy upon hydrogenation occurs in the two samples with the least hydrazine and most hydrocarbon, suggesting that the formation of hydride and loss of hydrocarbon is the key step in the increased enthalpies. These peak enthalpies are close to what is expected as a maximum in this system, as computations from our group have shown that transition metal hydrides can bind H_2 in a Kubas fashion with enthalpies as high as 60 kJ/mol.[25] This is somewhat higher than the 20−30 kJ/mol calculated as ideal for room temperature performance, but it is reasonable to assume that the system functions as an average over the rising trend and not at the peak. While the enthalpies for the 1.5 and 2.0 samples are lower than those for the 0.5 and 1.0, the room temperature excess storage is similar. The reason for this is likely due to a combination of high enthalpies and available binding sites, those materials with more hydrazine having a greater concentration of binding sites, and those with less hydrazine possessing higher enthalpies.

A 20-cycle run of adsorption and desorption at 298 K and with pressure up to 85 atm was carried out on H_2−Cr−MHz (1.5) as

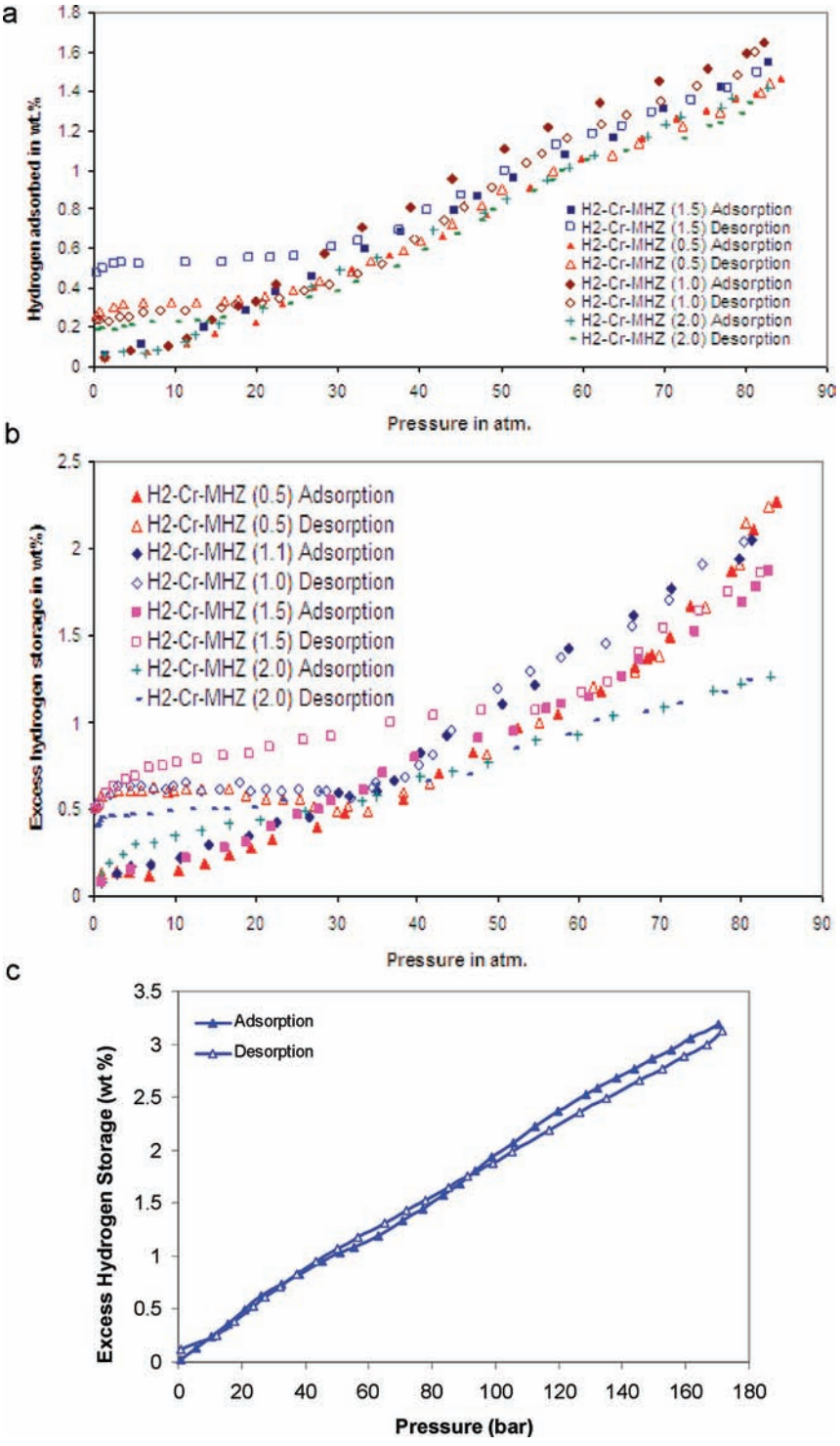

Figure 5. (a) Excess storage isotherms at 298 K of Cr−hydrazides prepared with various Cr:N_2H_4 ratios after hydrogenation at 180 °C and 85 atm for 4 h. (b) Excess storage isotherms at 77 K of Cr−hydrazides prepared with various Cr:N_2H_4 ratios after hydrogenation. (c) Excess storage isotherm of Cr−MHz (1.5) after hydrogenation at 180 °C recorded at 298 K measured up to 170 bar.

shown in Figure S20. There was no excess storage loss between the first and the last run. The adsorption results from all of the runs were in the range 1.49−1.59 wt %, which corresponds to the excess storage capacity ± the instrumental error. This indicates that the slight lack of reversibility at pressures less than 20 bar in some samples is a kinetic effect and that the materials show 100% reversibility within the context of the experimental life cycle and that the small amount of residual hydrogen desorbs easily during the purge cycle of the instrument.

The confirmation of Kubas binding to framework sites in hydrogen storage materials such as MOFs has so far been elusive. Metal binding sites in MOFs thought to function via a $\sigma-\pi$

dx.doi.org/10.1021/ja2021944 |*J. Am. Chem. Soc.* 2011, 133, 15434–15443

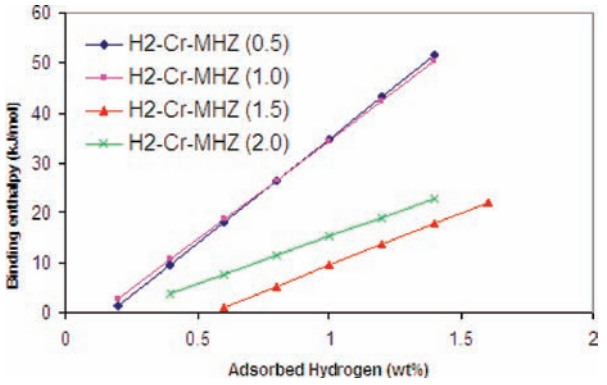

Figure 6. Binding enthalpies of chromium hydrazides prepared with various Cr:N_2H_4 ratios after hydrogenation.

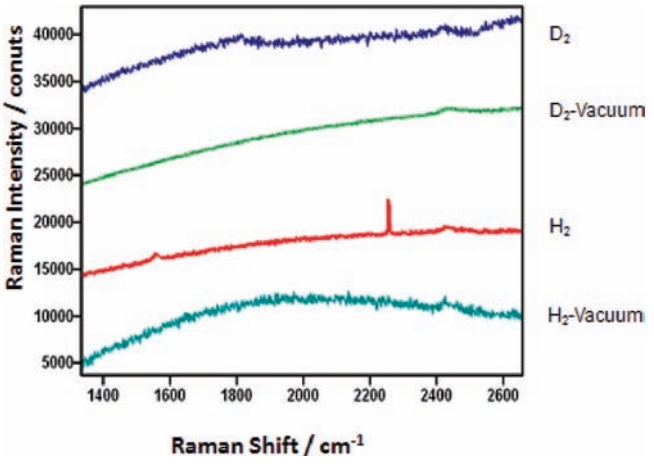

Figure 7. Raman spectra of Cr−MHz (1.5) under H_2 (green), under H_2 but after vacuuming (red), and under D_2.

interaction were later shown to be purely σ in nature.[3] Previous work from our group has suggested a Kubas interaction in materials with low-coordinate transition metal fragments supported on silica;[16] however, spectroscopic studies on these materials have not yet been conducted due to the small amount of active metal and the instability of the surface species. In a previous paper, we used electron paramagnetic resonance (EPR) spectroscopy to confirm the binding of H_2 to a V(III) center in a vanadium hydrazide material;[18] however, the intimate nature of this binding was not established. To date, the only clear examples of Kubas binding in porous networks have been in Cu-ZSM5, in which vibrational spectroscopy and inelastic neutron scattering were used to show a weak $\sigma-\pi$ interaction on the Cu center.[28] An H−H stretch is Raman active but formerly forbidden in IR spectroscopy, but it becomes allowed when coordinated to a metal because of polarization.[29] However, in practice, it is often weak or invisible in the IR unless coupled to vibrations of other ligands such as CO or phosphines. Figure 7 shows the Raman spectrum under H_2 for H_2−Cr−MHz (1.5). The sharp Raman band at 2280 cm^{-1}, falling exactly in the 2200−2700 cm^{-1} range for an M(H_2) H−H stretch,[29,30] is accompanied by a second much weaker scattering band at 1540 cm^{-1} that can be assigned to the M(H_2) M−H stretch by comparison with the spectrum for $W(CO)_3(PCy_3)_2(\eta_2\text{-}H_2)$.[29] Neither of the two Raman bands are observed in the IR spectrum of these materials, and both Raman signals vanish on application of vacuum. A recent study from our group has revealed Kubas binding of H_2 to V(III) oxamide polymers, with a M(H_2) H−H stretch at 2553 cm^{-1}.[31] For comparison, physisorbed H_2 has a Raman stretch above 4100 cm^{-1} on an MOF surface.[32] Backfilling the tube with D_2 leads to a new broad and weaker absorbance at 1798 cm^{-1} without reappearance of the two scattering bands observed for coordinated H_2. This new D_2 Raman band falls in the expected range for a M(D_2) D−D stretch in a Kubas complex[29] and vanishes on application of vacuum. In the IR spectrum of $W(CO)_3(PCy_3)_2(\eta_2\text{-}D_2)$, the M($D_2$) D−D stretch was also weaker than the corresponding H−H stretch.[29] The metal hydride stretch observed in the IR of the Cr materials does not appear in the Raman, but does not wash out over 5 h under D_2, indicating that there is no exchange between D_2 and the Cr−H. These experiments are consistent with Kubas binding of H_2 to the Cr centers as expected from previous work in our group and establish the mechanism of hydrogen binding in this system, while also tying the rising enthalpy trends in this and our previous work[16−18,25] to the Kubas interaction.

CONCLUSIONS

New materials containing an extended network of low coordinate chromium metal centers for Kubas-type hydrogen storage were designed and synthesized by treating bis[(trimethylsilyl) methyl]chromium(II) with hydrazine followed by thermal treatment and subsequent hydrogenation. After hydrogenation, there was a 3−6-fold increase in the excess storage capacity at 298 K, which reaches a high of 3.2 wt % at 170 bar without saturation, with an absolute volumetric density of 40.8 kg/m^3, in the range of the 2015 DOE system target for volumetric storage. The improved performance is attributed to an increase in the binding enthalpies of the Cr center as a result of the substitution of the Cr−[(trimethylsilyl) methyl] moieties with Cr−H moieties. Raman spectroscopy under H_2 and D_2 confirmed the binding mechanism in these materials as nonclassical Kubas type binding. Because 170 bar is a safe operating pressure and these materials possess moderate enthalpies that allow for room temperature use without excess heat management problems that require exotic and expensive tanks for on-board use, these or related next-generation materials may offer an ideal solution to chemical hydrogen storage.

ASSOCIATED CONTENT

Supporting Information. Elemental analysis results, nitrogen surface areas, powder X-ray diffraction spectra, infrared spectra, X-ray photoelectron spectra in Cr 2p and N 1s region of all materials; and 20-cycle adsorption and desorption of H2−Cr−MHz (1.5) at room temperature. This material is available free of charge via the Internet at http://pubs.acs.org.

AUTHOR INFORMATION

Corresponding Author
dantonel@glam.ac.uk

ACKNOWLEDGMENT

NSERC is acknowledged for funding.

REFERENCES

(1) Schlapbach, L.; Zuettel, A. *Nature* **2001**, *414*, 353.
(2) Seayad, A. M.; Antonelli, D. M. *Adv. Mater.* **2004**, *16*, 765.
(3) Murray, L. J.; Dinca, M.; Long, J. R. *Chem. Soc. Rev.* **2009**, *38*, 1294.
(4) Thomas, K. M. *Dalton Trans.* **2009**, 1487.
(5) Rowsell, J. L. C.; Yaghi, O. M. *Angew. Chem., Int. Ed.* **2005**, *44*, 4670.
(6) Dinca, M.; Long, J. R. *Angew. Chem., Int. Ed.* **2008**, *47*, 6766.
(7) Hamilton, C. W.; Baker, R. T.; Staubitz, A.; Manners, I. *Chem. Soc. Rev.* **2009**, *38*, 279.
(8) Orimo, S.; Nakamori, Y.; Eliseo, J. R.; Zuettel, A.; Jensen, C. M. *Chem. Rev.* **2007**, *107*, 4111.
(9) DOE Target for Onboard Hydrogen Storage Systems for Light-Duty Vehicles.
(10) http://www1.eere.energy.gov/hydrogenandfuelcells/storage/pdfs/targets_onboard_hydro_storage.pdf. Retrieved on March 9, 2011.
(11) Lochan, R. C.; Head-Gordon, M. *Phys. Chem. Chem. Phys.* **2006**, *8*, 1357.
(12) Bhatia, S. K.; Myers, A. L. *Langmuir* **2006**, *22*, 1688.
(13) Kubas, G. J. *Chem. Rev.* **2007**, *107*, 4152.
(14) Zhao, Y. F.; Kim, Y. H.; Dillon, A. C.; Heben, M. J.; Zhang, S. B. *Phys. Rev. Lett.* **2005**, *94*, 155504.
(15) Hoang, T. K. A.; Antonelli, D. M. *Adv. Mater.* **2009**, *21*, 1787.
(16) Hamaed, A.; Trudeau, M.; Antonelli, D. M. *J. Am. Chem. Soc.* **2008**, *130*, 6992.
(17) Mai, H. V.; Hoang, T. K. A.; Hamaed, A.; Trudeau, M.; Antonelli, D. M. *Chem. Commun.* **2010**, *46*, 3206.
(18) Hoang, T. K. A.; Webb, M. I.; Mai, H. V.; Hamaed, A.; Walsby, C. J.; Trudeau, M.; Antonelli, D. M. *J. Am. Chem. Soc.* **2010**, *132*, 11792.
(19) Schulzke, C.; Enright, D.; Sugiyama, H.; LeBlanc, G.; Gambarotta, S.; Yap, G. P. A. *Organometallics* **2002**, *21*, 3810.
(20) Schmidt, E. W. *Hydrazine and its Derivatives: Preparation, Properties, Application*; John Wiley & Sons, Inc.: New York, 2001.
(21) Hu, X.; Skadtchenko, B. O.; Trudeau, M.; Antonelli, D. M. *J. Am. Chem. Soc.* **2006**, *128*, 11740.
(22) Furukawa, H.; Miller, M. A.; Yaghi, O. M. *J. Mater. Chem.* **2007**, *17*, 3197.
(23) Roquerol, F.; Roquerol, J.; Sing, K. *Adsorption by Powders and Solids: Principles, Methodology, and Applications*; Academic Press: London, 1999.
(24) Antonelli, D. M.; Schaefer, W. P.; Parkin, G.; Bercaw, J. E. *J. Organomet. Chem.* **1993**, *462*, 213.
(25) (a) Skipper, C. V. J.; Hamaed, A.; Antonelli, D. M.; Kaltsoyannis, N. *J. Am. Chem. Soc.* **2010**, *132*, 17296. (b) Skipper, C. V. J.; Hoang, T. K. A.; Antonelli, D. M.; Kaltsoyannis, N. *Chem. —Eur. J.* **2011**, submitted.
(26) Li, Y.; Yang, R. T. *Langmuir* **2007**, *23*, 12937.
(27) Zuettel, A., Borgschutle, A., Schlapbach, L., Eds. *Hydrogen as a Future Energy Carrier*; Wiley-VCH: Weinheim, 2008.
(28) Georgiev, P. A.; Albinati, A.; Mojet, B. L.; Ollivier, J.; Eckert, J. *J. Am. Chem. Soc.* **2007**, *129*, 8086.
(29) Bender, B. R.; Kubas, G. J.; Jones, L. H.; Swanson, B. I.; Eckert, J.; Capps, K. B.; Hoff, C. D. *J. Am. Chem. Soc.* **1997**, *119*, 9179.
(30) Stone, F. G. A.; West, R. *Advances in Organometallic Chemistry*; Academic Press: London, 1988; Vol. 38, p 303.
(31) Hoang, T. K. A.; Hamaed, A.; Moula, G.; Aroca, R.; Trudeau, M.; Antonelli, D. M. *J. Am. Chem. Soc.* **2011**, *133*, 4955.
(32) Centrone, A.; Siberio-Perez, D. Y.; Millward, A. R.; Yaghi, O. M.; Matzger, A. J.; Zerbi, G. *Chem. Phys. Lett.* **2005**, *411*, 516.